Scientia Iranica A (2013) 20 (3), 431–444

Sharif University of Technology

Scientia Iranica

Transactions A: Civil Engineering

www.sciencedirect.com

Nonlinear seismic assessment of steel moment frames using time–history, incremental dynamic, and endurance time analysis methods

M.A. Hariri-Ardebili [a,*], Y. Zarringhalam [b], H.E. Estekanchi [c], M. Yahyai [b]

[a] *Department of Civil Environmental and Architectural Engineering, University of Colorado at Boulder, UBC, P.O. Box 80309-0428, Boulder, CO, USA*

[b] *Department of Civil Engineering, K.N. Toosi University of Technology, P.O. Box 15875-4416, Tehran, Iran*

[c] *Department of Civil Engineering, Sharif University of Technology, P.O. Box 11155-9313, Tehran, Iran*

Received 22 January 2012; revised 10 November 2012; accepted 23 December 2012

KEYWORDS

Endurance time analysis;
Incremental dynamic analysis;
Steel moment resisting frames;
Nonlinear seismic assessment.

Abstract A recent method in the seismic assessment of structures is Endurance Time Analysis (ETA). ETA is a time–history-based dynamic pushover procedure, in which structures are subjected to gradually intensifying acceleration functions called Endurance Time Acceleration Functions (ETAFs), and their performances are evaluated based on the equivalent intensity level that they can endure while satisfying required performance goals. In this paper, the accuracy of the ETA in the seismic assessment of steel moment resisting frames is compared with the Time History Analysis (THA) and Incremental Dynamic Analysis (IDA) methods. For this purpose, a set of mid-rise and high-rise frames were selected as a case study. Three sets of second generation ETAFs were used as input in the ETA method, and seven scaled ground motions were used for THA and IDA. It was found that ETA can estimate THA results in an equivalent target time, and also the general trend of IDA curves, with acceptable accuracy, while ETA requires considerably less computational effort in comparison with THA, and, especially, the IDA method.

1. Introduction

Performance Based Earthquake Engineering (PBEE) procedures require prediction of the seismic capacity of structures when subjected to different levels of ground shaking, which is then compared to the local seismic demand. The interrelationship between the two gives an inference of the expected level of damage for a given level of ground shaking. Limitations of traditional seismic analysis procedures and also progress in computational technology have encouraged researchers to develop other analysis methods, such as pushover analysis (POA) [1,2] and Incremental Dynamic Analysis (IDA) [3–5]. Although methods such as IDA can describe the seismic behavior of structures more precisely, the necessity for large numbers of nonlinear analyses and the difficulty in interpretation of the results have led to limitation in the usage of this method, only being used for very important structures and special cases. So, the creation of a new analysis method, which is able to both estimate the real behavior of the structural systems with high accuracy identical to IDA and be less time consuming, has become an important challenge [6,7]. The Endurance Time Analysis (ETA) method was introduced by Estekanchi et al. [8], where a heuristic method was used in order to produce intensifying seismic inputs called Endurance Time Acceleration Functions (ETAFs), which are the basis of the analysis in this method. ETA is a special method capable of estimating various responses of structures from low to high excitation levels in a single analysis. The average of several analyses can be used in order to reduce uncertainties in this method [9–11].

Application of ETA in linear seismic analysis of structures has been studied before [9]. In this study, a-series of ETAFs have been applied to various steel moment and braced frames,

* Corresponding author. Tel.: +1 303 492 7459.
E-mail addresses: mohammad.haririardebili@calorado.edu (M.A. Hariri-Ardebili), yashar-zarringhalam@sina.kntu.ac.ir (Y. Zarringhalam), stkanchi@sharif.edu (H.E. Estekanchi), yahyai@kntu.ac.ir (M. Yahyai).

Peer review under responsibility of Sharif University of Technology.

Production and hosting by Elsevier

which were designed based on the Iranian National Building Code and the results of analysis were compared to conventional equivalent static and response spectrum seismic analysis procedures. It was found that story drifts and internal forces from the ET method are consistent with response spectrum analysis and static analysis results within acceptable tolerances. Also, Estekanchi et al. studied various damage indexes in the ETA method, as the endurance criteria, and compared results with nonlinear THA [12]. In this investigation, correlation between the values of various damage indexes, as obtained from nonlinear THA of steel moment frames subjected to scaled earthquakes, is compared with that of the ETA method at the same level of spectral acceleration. It was found that the average value of various damage indexes can be estimated from ETA results. Emamjome and Estekanchi compared the results of IDA with ETA for a set of SDOF and MDOF structures [13]. In this research, they selected several SDOF systems with different periods and yield force and also various low-rise to mid-rise steel frames as MDOF systems. They conclude that by considering spectral acceleration as the Intensity Measure (IM), ETA can predict IDA results with reasonably good accuracy. In another study, Arjomandi and Estekanchi [14] studied various damage indices of steel frames in an analysis based on the ETA method. They also compared how damage was developed due to real ground motion and ETAFs. They found that ETA and IDA methods were consistent in predicting the relative drift of a roof in steel frames, but there was no meaningful correlation in the prediction of failure using cyclic damage indices [15]. Hariri et al. [6] compared ETA and IDA methods for a set of steel frames. They compared not only the general trend of IDA and ETA curves, but also the estimated capacities in various limit-states. Finally, they conclude that ETA is capable of identifying mean results of the IDA method.

Application of the ETA method in nonlinear analysis of SDOF systems was investigated by Riahi et al. [16]. In this study, they compared the results of ETA with real ground motions analysis results at different strength ratio, ductility and damping ratios. Also, they considered the effects of stiffness degeneration and strength deterioration in the studies. They showed that the results of the ETA method are in good agreement with the exact response history results of similar ground motions. In another study, Estekanchi et al. investigated the accuracy of the ETA method in estimating average deformation demands of low and medium rise steel frames using the f-series of ETAFs [17]. In this study, an elastic-perfectly-plastic model, and also a bilinear material model were considered. It was shown that, although the results of the ETA are not exactly consistent with the results of ground motions analysis, the ETA method can clearly identify the structure with a better performance, even in the case of structures with a relatively complicated nonlinear behavior.

In the present study, we will undertake a brief review of the concept of ETA and IDA methods. Properties of ETAFs with various durations are studied and the methodology for comparison of results between ETA and IDA, as well as ETA and THA, are proposed. For the case study, a set of Steel Moment Resisting Frames (SMRFs) with different story numbers were used. A plastic hinge model was used for simulation of nonlinear behavior in all frames. Plastic-hinge models for beam–columns have a tri-linear backbone curve, considering strength loss, with a post-yield stiffness equal to 3% of the initial elastic stiffness. Results of analyses are compared in story shear and interstory drift ratio for different frames.

2. Concept of endurance time analysis method

The ETA method is a dynamic pushover procedure for predicting the seismic performance of structures by analyzing their resilience when subjected to predesigned intensifying dynamic excitations [8]. In this method, numerical or experimental models of structures (or systems) are subjected to intensifying dynamic acceleration. Structural responses, such as displacements, accelerations, stresses, forces or other appropriate Damage Measures (DMs), are monitored up to the point where the structure collapses or analysis does not converge. The time duration from the start of the analysis to this collapse point is called the collapse endurance time [12]. Basically, the longer the structure can endure imposed excitations, it is judged to have a better performance. In practice, the objective of the analysis does not need to be limited to the collapse capacity, and any convenient performance parameter, such as maximum displacement, stress ratio and so on, can be considered at various excitation levels. Analysis or experiment can be commenced until the desired level of excitation has been covered [8,18]. Although, at a first view, there are some similarities between ETA and POA, ETA is capable of analyzing any type of structure (dams, bridges, offshore structures $\cdots$) with any kind of material complexity and irregularity, just like the THA, the application of POA is mainly limited to framed structures with a set of assumptions for simplification of the problem.

The concept of ETA can be described using hypothetical shaking table experiments on simple frames [19]. Three different structures with unknown structural properties are to be ranked according to their seismic resistance performance. All three structures are fixed on a shaking table and the test begins by subjecting the structures to an increasing acceleration function, as shown in Figure 1. As time passes, the amplitude of vibrations is increased in the shaking table.

As the vibration amplitude increases, at a particular time, say at $t = t_1$ in this hypothetical experiment, one of the structures, say structure "A", fails, as shown in Figure 1. Afterwards, as the amplitude of vibration is increased, at $t = t_2$ and $t = t_3$, the second and third structures also fail, i.e. structures "C" and "B", respectively, in this case. Based on these results and assuming that the lateral loads induced by the shaking table can somehow be correlated with earthquake induced loads, structure "A", which failed earliest, can be ranked as the worst, and structure "B", which endured longest, can be ranked as the best. This hypothetical experiment describes the essence of the ETA method.

Numerically, after simulating an appropriate finite element model of physical phenomenon and specifying a suitable Damage Index (DI), ETA can be run using appropriate ETAFs, and the selected DI time history is recorded during analysis. The maximum absolute value of DI is plotted for the total duration of the analysis. Then, the Endurance Time Analysis (ETA) curve is plotted for each DI or response of the system. In theory, the ETA curve represents a special diagram, whose vertical axis values refer to the maximum absolute values of DI during the time interval from 0.0 to t, based on Eq. (1):

$$\Omega\left(f\left(t\right)\right) \equiv \mathrm{Max}\left(Abs\left(f\left(\tau\right) : \tau \in [0, t]\right)\right), \tag{1}$$

in which Ω acts as maximum absolute operator and $f(t)$ represents the time history of the considered response. Hypothetical ETA curves for frames in Figure 1 are depicted in Figure 2. As can be seen, for the same DI (for example, maximum allowable roof drift, in this example) frame "B" has the longest endurance time (about 17.5 s) and frame "A" has the shortest endurance time (about 13.0 s).

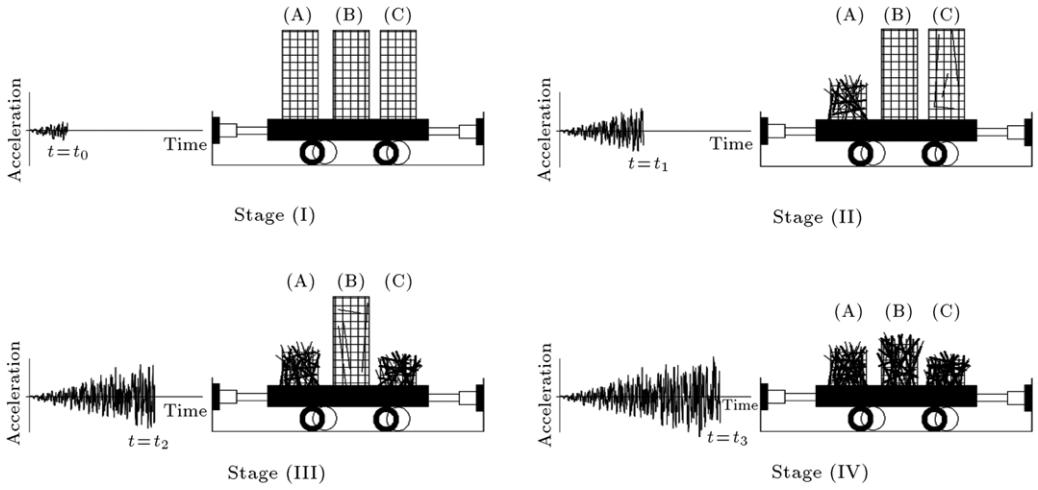

Figure 1: Schematic of hypothetical shaking table experiment on frames (Stages I–IV).

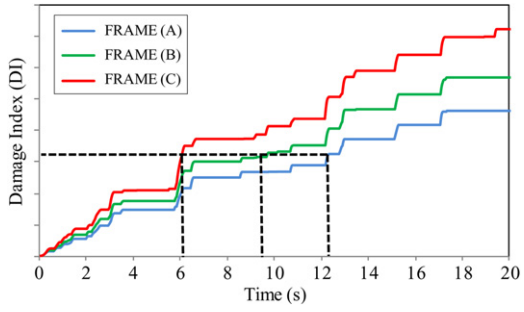

Figure 2: Hypothetical ETA curves for frames shown in Figure 1.

2.1. Characteristics of ETAFs

The first generation of acceleration functions was produced using random numbers with a Gaussian distribution of zero mean and a variance of unity [8,20]. In this method, the stimulator function is defined as a finite sum of harmonic functions as:

$$a(t) = \sum_{i=1}^{N} A_i \cdot \sin(\omega_i t + \phi_i), \tag{2}$$

where $a(t)$ is the acceleration function, N is the number of acceleration points, ω_i is the angular frequency of the ith term, φ_i is the angle of phase delay in the sinusoidal component and A_i is Fourier amplitude. If amplitudes and the angle of phase delay in the sinusoidal component is supposed as a vector form, it is possible to generate different functions by the constant amplitude and fluctuating angle of the phase delay. All generated functions produced by this method are stationary and ergodic. A stationary random acceleration function was generated using $\delta t = 0.01$ and $n = 2^{11} = 2048$, with PGA = 1.0 g. So, the duration of the acceleration function was equal to $\delta t \times n = 20.48$ s.

The frequency content of the random acceleration functions that was statistically similar to a white noise was then modified, in order to resemble real earthquake accelerograms. For this purpose, filter functions were applied to the random acceleration functions, as explained by Clough and Penzien [20]. The frequency content was then further modified in order to generate acceleration functions with response spectra that are compatible with typical seismic code responses. For this purpose, the response spectra of the Iranian National Building Code (INBC) [21] had been used as a sample. In the next step, the acceleration values were adjusted for target values of velocity and acceleration. Finally, the acceleration values were multiplied by a linear profile function ($g(t) = t/10$). Three acceleration functions were generated and named acc1, acc2 and acc3. The term 'First Generation' is predicated to acc1–3 acceleration functions, because they were generated using a heuristic approach without direct control over response parameters. These ETAFs were useful in demonstrating the concept of applying an intensifying excitation to structures, but, as expected, they produced poor numerical estimations [8].

In order to improving general characteristics of acceleration functions and improving them for practical structural engineering applications, a 'Second Generation' of ETAFs was produced [22]. In this generation, in order for the ETAFs to somehow correspond to average code compliant design level earthquakes, the concept of the response spectrum has been more directly involved. Like the first generation, a linear intensifying pattern was chosen for this set and designed in such a way as to produce dynamic responses equal to the code's design spectrum at a predefined time, t_{eq}, and a time proportional response spectrum at all other times. In this way, the target spectral acceleration and displacement are defined as a function of time and period, as follows [9]:

$$\begin{cases} S_a^{ET}(t,T) = \dfrac{t}{t_{eq_\bullet}} S_a^{TARGET}(T) \\ S_u^{ET}(t,T) = \dfrac{t}{t_{eq_\bullet}} S_a^{TARGET}(T) \times \left(\dfrac{T}{2\pi}\right)^2 \end{cases} \tag{3}$$

where $S_a^{ET}(t,T)$ and $S_u^{ET}(t,T)$ are ETAFs target acceleration and displacement response values at time t, $S_a^{TARGET}(T)$ is target acceleration responses of the structure and T is the period of free vibration. Considering that an analytical approach to finding an ETAF that satisfies Eq. (3) is formidably complicated, a numerical optimization technique was used to solve it using the following formulation [11,22]:

$$\min_{a_g} F(a_g) = \int_0^{T_{\max}} \int_0^{t_{\max}} \left\{ \left[S_a^{ET}(t,T) - S_a(t,T)\right]^2 + \alpha \left[S_u^{ET}(t,T) - S_u(t,T)\right]^2 \right\} dt\, dT \tag{4}$$

Table 1: Characteristics of GM1 set of ground motions and corresponding scale factors.

Abbreviation	Earthquake name and date	Station no.	Selected component	Magnitude (Ms)	PGA (cm/s^2)	Scale factor
LADSP000	Landers (06/28/1992)	12 149	0	7.5	167.8	3.650
LPSTG000	Loma Prieta (10/17/1989)	58 065	0	7.1	494.5	1.450
LPGIL067	Loma Prieta (10/17/1989)	47 006	67	7.1	349.1	2.220
LPLOB000	Loma Prieta (10/17/1989)	58 135	360	7.1	433.1	2.300
LPAND270	Loma Prieta (10/17/1989)	1 652	270	7.1	239.4	2.625
MHG06090	Morgan Hill (04/24/1984)	57 383	90	6.1	280.4	1.850
NRORR360	North Ridge (01/17/1994)	24 278	360	6.8	504.2	1.095

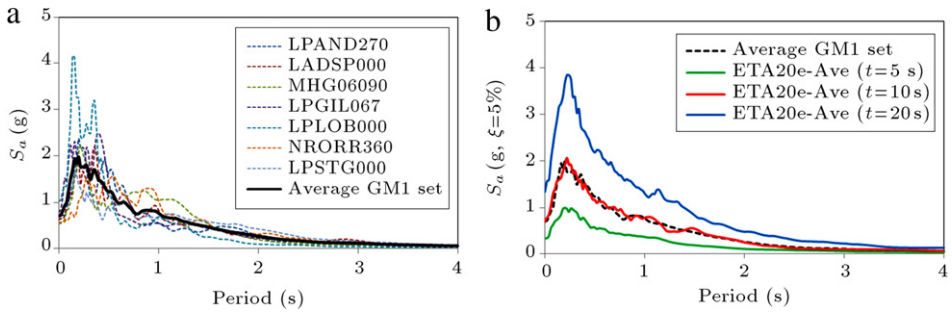

Figure 3: Acceleration response spectrum (a) seven scaled ground motions of GM1 set and their average; (b) average of ETA20e01-03 in various time intervals.

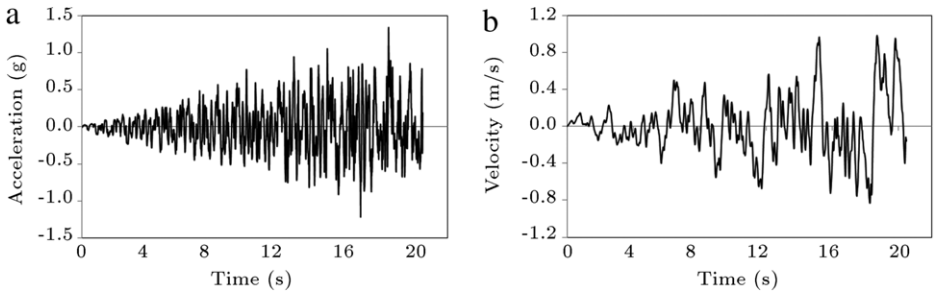

Figure 4: (a) Typical ETAF from *e*-series, (b) corresponding ETVF from *e*-series.

where a_g is the acceleration function being sought and α is a weighting parameter. Starting from a randomly generated acceleration function, unconstrained optimization can be used to solve the problem. The first three ETAFs that have been generated by this method are called as ETA20a01-03 (*a*-series). It is worth noting that the base target time has been assumed 10 s in generation of this set, i.e. the ETAFs response spectrum reaches the standard code level at $t = 10$ s with a scale factor of unity. At all other times, in effect, a time proportional scale factor has been applied.

To investigate the potential of the ETA method in comparison with THA and IDA methods, a set of ETAFs, called ETA20e01-03 (ETA20f01-03 and ETA20h01-03), are used in the present paper. These sets are also referred to as *e*-, *f*- and *h*-series, each consisting of three ETAFs generated using the above formulation but with different target spectra. In these series, 20 accelerograms, which were defined by the NEHRP and used in FEMA-440 [23], were selected as base ground motions. From these ground motions, seven records, whose response spectra shapes were more compatible with the response spectrum of soil type II of INBC [21], were selected [17] (Table 1). These seven accelerograms, which are called the GM1 set, were scaled to produce a response spectrum compatible with the INBC spectrum. Finally, the average of the pseudo acceleration spectrum of these scaled accelerograms is obtained and smoothed (Figure 3(a)). The smoothed spectrum was used as the base target spectrum in generating these sets of ETAFs (Figure 3(b)). These ETAFs were generated in such a way that their response spectra increased by time. Hence, the response of the structure under these kinds of accelerogram gradually increases with time. A typical ETAF from this family is depicted in Figure 4(a). As obvious, Peak Ground Acceleration (PGA) increases in an almost linear trend with time passage. The Endurance Time Velocity Function (ETVF) for the considered ETAF is depicted in Figure 4(b). Series *e*- and *f*-are identical; statistically equivalent. The *h*-series, however, is of double duration, i.e. 40 s, used when higher intensity and duration are required.

Figure 3(b) also presents the response spectrum of the average of the ETAFs (*e*-series) at various times. This set has been generated in a manner in which its response spectrum at the base target time, which is taken to be 10 s, is matched with the base target response spectrum used for generation of the *e*-series (GM1 set) with a scale factor of unity [17]. It is worthy to note that the ETAF response spectrum remains linearly proportional to the target spectrum at all times. For example, the response spectrum for the average of ETAFs at time $t = 10$ s is twice that of the response spectrum at time $t = 5$ s and half of that at time $t = 20$ s (Figure 3(b)) [24].

3. Comparison methodology

3.1. Comparison between ETA and THA

The ETA method is capable of estimating the responses of a system that can be similarly obtained by the THA method. This method predicts linear and nonlinear responses of systems with reasonably high accuracy, using currently available ETAFs. In the present study, to compare the results of ETA with real earthquake ground motion, the GM1 set is used in THA. In order to be consistent with the seismic code, the GM1 set of ground motions should be scaled as per code recommendations. Considering that in the present study only a single horizontal component of ground motion is used in the analysis of frames, records are scaled individually. For this purpose, it is supposed that the average of 5% damped linear response spectra does not fall below the design spectrum for the period range $0.2T_i$ to $1.5T_i$, where T_i is the fundamental period of vibration of each frame modeled as a linear system. Here, scale factors are obtained in such a way that the ground motion spectrum matches the design spectrum in the mentioned range.

Because of the intensifying nature of ETAFs, it is questionable as to how the results of two methods can be compared with each other. As is clear, in the ETA method, the time is correlated with intensity and different responses of the structure are calculated for various values of dynamic load intensity in an ETA. To establish a relationship between the results of the ETA and THA methods, the intensity value of the THA should be found in the ETA. Therefore, a procedure should be defined to find an equivalent target time in the ETA, in which the intensity values of the two methods are equal. Various quantities can be used to characterize the intensity of a ground motion record, i.e. Peak Ground Acceleration (PGA), Peak Ground Velocity (PGV) and spectral acceleration, at the structure's first-mode period ($S_a(T_1)$). In the present section, $S_a(T_1)$ is used as the dynamic load intensity to obtain the equivalent target time.

The equivalent target time can be calculated for a single record or a set of records. In the proposed technique, in the current study, the 10th second of ETAFs is selected as the base target time, and, therefore, the average response spectrum resulted up to the 10th second of ETAFs is interpreted as the base response spectrum (which corresponds with the base target response spectrum for the generation of ETAFs). Consequently, the equivalent target time is calculated by multiplying the ψ factor, called the spectrum ratio, in constant 10, as shown in Eq. (5):

$$t_{eq}(T_R) = \psi(T_R, T_{eff}) \times 10, \tag{5}$$

in which $t_{eq}(T_R)$ is the equivalent target time for the desired performance level (or design spectrum), with return period T_R, and $\psi(T_R, T_{eff})$ is the spectrum ratio with return period T_R, and for an effective period interval equal to T_{eff}. In the present study, the spectrum ratio is calculated as follows:

$$\psi(T_R, T_{eff}) = \frac{S_a^{T_R,T_n}}{S_a^{ET,T_n}}, \tag{6}$$

where $S_a^{T_R,T_n}$ is average of the spectral acceleration of the seven ground motions at the first-mode period (fundamental period) and S_a^{ET,T_n} is the value of the smooth response spectrum used for the generation of ETAFs at the first-mode period. In fact, the calculated equivalent target time for each frame (or system) shows that the results obtained from the average of ETA up to the calculated time should have the same, or as close a value, as the average maximum values resulted from THA from seven ground motions.

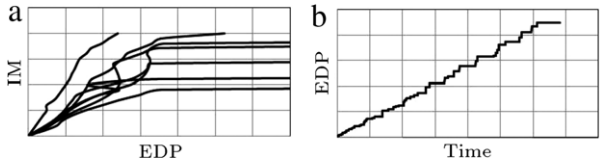

Figure 5: Schematic of IDA curve (a) and ETA curve (b).

3.2. Comparison between ETA and IDA

In order to compare the results of the ETA method with IDA, it is required that various parameters in the ETA method be converted to appropriate equivalent parameters in the IDA method. Two important factors in the IDA method are the selection of the appropriate IM and Engineering Demand Parameter (EDP) during analyses. Then, the IDA curve can be plotted in the IM-EDP coordinate system. In the present study, PGA is selected as IM, and, in addition, maximum interstory drift ratio and base shear are selected as EDPs in the IDA method. On the other hand, as mentioned before, in the ETA curve, main factors are time and EDP, which are plotted in the EDP-Time coordinate system. The schematic of IDA and ETA curves are depicted in Figure 5. As is clear, EDP is a similar parameter in both methods, so it is just required that the "Time" parameter in ETA method be converted appropriately to similar IM in the IDA method, which is "PGA" in the present study. This conversion can be easily done by considering the envelope of the acceleration time history for each ETAF. In this technique, each time like t_1 corresponds with the specific PGA value experienced by the system between time intervals 0 to t_1. The second step is to inverse the EDP-Time coordinate system to obtain the Time-EDP coordinate system, which is consistent with standard engineering practice, where the independent variable is plotted on the vertical axis. Finally, both general trends of the curve in the two methods, and also the capacities in various limit-states, can be compared between ETA and IDA.

4. Numerical models of structures and materials

A set of Steel Moment Resisting Frames (SMRFs) with different numbers of stories was selected for case studies. This set consists of 2D regular frames with 9, 11, 13 and 15 stories and three bays, which are categorized as mid-rise and high-rise frames. The height of all stories is 3.0 m and the width of the bay frame is 5.0 m. These frames are designed according to the UBC-97 design code [25]. All considered frames are classified in group 4 of the occupancy category, based on UBC-97, and, therefore, the seismic importance coefficient is set to one in these frames. The main purpose in the design of such structures is to minimize loss of life under earthquake ground motion with a 475-year return period (10% probability of occurrence in 50 year). It means that based on FEMA-356 [26], the Life Safety (LS) performance level should be satisfied under this condition. It is noteworthy that in order to consider the stiffness effects of infill panels and also non-structural components of the structure, the stronger sections were considered in the present analyses, rather than the designed sections, so that the first mode period of the simulated model was close to the analytical period in the code. The section properties of all frames and their characteristics are depicted in Figure 6. Also, yield stress is considered to be 240 MPa and ultimate stress is 400 MPa.

The tri-linear material model, with a post-yield stiffness equal to 3% of the initial elastic stiffness, and considering the

STORIES	15	IPB 360	IPE 360						
	14	IPB 360	IPE 360						
	13	IPB 360	IPE 360	IPB 360	IPE 360				
	12	IPB 360	IPE 400	IPB 360	IPE 360				
	11	IPB 360	IPE 400	IPB 360	IPE 360	IPB 360	IPE 360		
	10	IPB 400	IPE 400	IPB 360	IPE 400	IPB 360	IPE 360		
	9	IPB 400	IPE 450	IPB 360	IPE 400	IPB 360	IPE 360	IPB 360	IPE 360
	8	IPB 450	IPE 450	IPB 400	IPE 400	IPB 360	IPE 400	IPB 360	IPE 360
	7	IPB 450	IPE 450	IPB 400	IPE 450	IPB 360	IPE 400	IPB 360	IPE 360
	6	IPB 550	IPE 500	IPB 450	IPE 450	IPB 400	IPE 400	IPB 360	IPE 400
	5	IPB 600	IPE 500	IPB 450	IPE 450	IPB 400	IPE 450	IPB 360	IPE 400
	4	IPB 600	IPE 500	IPB 550	IPE 500	IPB 450	IPE 450	IPB 400	IPE 400
	3	IPB 700	IPE 500	IPB 600	IPE 500	IPB 450	IPE 450	IPB 400	IPE 450
	2	IPB 800	IPE 500	IPB 600	IPE 500	IPB 550	IPE 500	IPB 450	IPE 450
	1	IPB 900	IPE 500	IPB 700	IPE 500	IPB 600	IPE 500	IPB 450	IPE 450
Number of stories		Column	Beam	Column	Beam	Column	Beam	Column	Beam
		SMFR15@3		**SMFR13@3**		**SMFR11@3**		**SMFR09@3**	
Fundamental Period (sec)		**1.70**		**1.80**		**1.62**		**1.38**	
Mass participation of 1st mode		**69%**		**74%**		**75%**		**74%**	

Figure 6: Section properties and characteristics of frames.

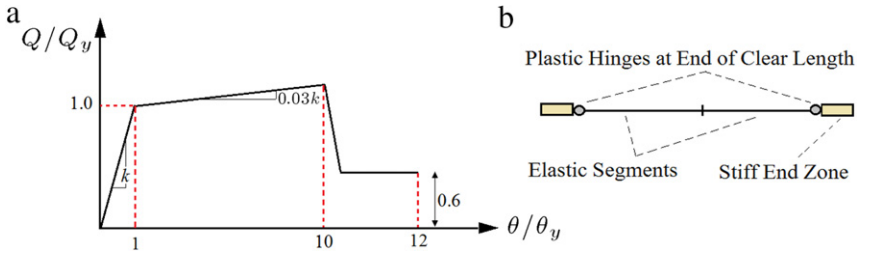

Figure 7: (a) Force–deflection relation for material model, (b) plastic hinge model in present study.

effects of strength loss, was used to study the nonlinear behavior of the frames (Figure 7(a)). This model has been used widely in previous investigations and, therefore, represents a benchmark to study the effect of hysteretic behavior. Furthermore, recent studies have shown that this is a reasonable hysteretic model for steel beams [27]. For more realistic nonlinear behavior, the chord rotation model is also used in this study [28]. This model is the easiest to use, and FEMA-356 gives some specific guidelines for this model. To apply these material models to the analysis, the *PERFORM* beam–column element with nonlinear lumped plasticity was utilized. The plastic deformations are concentrated to zero-length plastic hinges (Figure 7(b)) [28]. As mentioned previously, only one (horizontal) component of the ground motion has been considered in the present study, while dynamic soil–structure interaction has been neglected. $P-\Delta$ effects have been included in the analysis. A viscous damping of 5%, customary for these types of frame, has been applied to the analyses. This value of damping is also consistent with the value used for generating codified response spectra and ETAFs.

5. Results and discussion

5.1. ETA vs. THA

In the following subsections, the capability of the ETA method in estimating various parameters of THA, such as displacement, story shear and interstory drift ratio, has been studied. For analysis of frames based on the ETA method, *e*- and *f*-series of ETAFs have been used. Also, seven ground motions of the GM1 set are used in nonlinear THAs. To be consistent with seismic codes, the GM1 sets of ground motion are scaled individually. As mentioned before, the 5% damped linear response spectra for each ground motion should not fall below the design spectrum (UBC-97) for the period range $0.2T_i$ to $1.5T_i$. Scale factors obtained by this method for the GM1 set are shown in Table 2 for each frame. The calculated equivalent target times for each frame are shown in the last column of Table 2. Based on Table 2, the equivalent target time for SMRF09@3 is 12.64 s. It means that the average results from ETA up to 12.64 s should have the same as, or close to, the values of the average maximum results from THA using the GM1 set of ground motions. This procedure is also applicable in other frames.

For each set of Ground Motions (GM1) and ETAFs, the mean value and standard deviation of the specified EDP can be calculated. For example, for a set of ground motions, the mean value and standard deviation of the EDP can be worked out by Eqs. (7) and (8). Moreover, the percentage of errors between maximum average results in the ETA and THA methods is calculated using Eq. (9).

$$\overline{\mathrm{EDP}} = \frac{1}{n}\sum_{i=1}^{n}\mathrm{EDP}_i, \tag{7}$$

$$\sigma = \sqrt{\frac{\sum_{i=1}^{n}\left(\mathrm{EDP}_i - \overline{\mathrm{EDP}}\right)^2}{n-1}}, \tag{8}$$

$$Err\% = \left(\frac{\overline{\mathrm{EDP}}_{\mathrm{ETA}} - \overline{\mathrm{EDP}}_{\mathrm{THA}}}{\overline{\mathrm{EDP}}_{\mathrm{THA}}}\right) \times (100\%), \tag{9}$$

Table 2: Scale factors for GM1 set and calculated equivalent target time for each frame.

Frame	Scale factors							Equivalent target time (s)
	LADSP000	LPSTG000	LPGIL067	LPLOB000	LPAND270	MHG06090	NRORR360	
SMRF15@3	7.019	2.346	3.366	2.669	4.923	4.113	2.339	17.63
SMRF13@3	7.017	2.343	3.361	2.664	4.917	4.109	2.334	18.06
SMRF11@3	5.848	1.953	2.801	2.220	4.098	3.4246	1.945	14.71
SMRF09@3	4.678	1.562	2.241	1.776	3.278	2.739	1.556	12.64

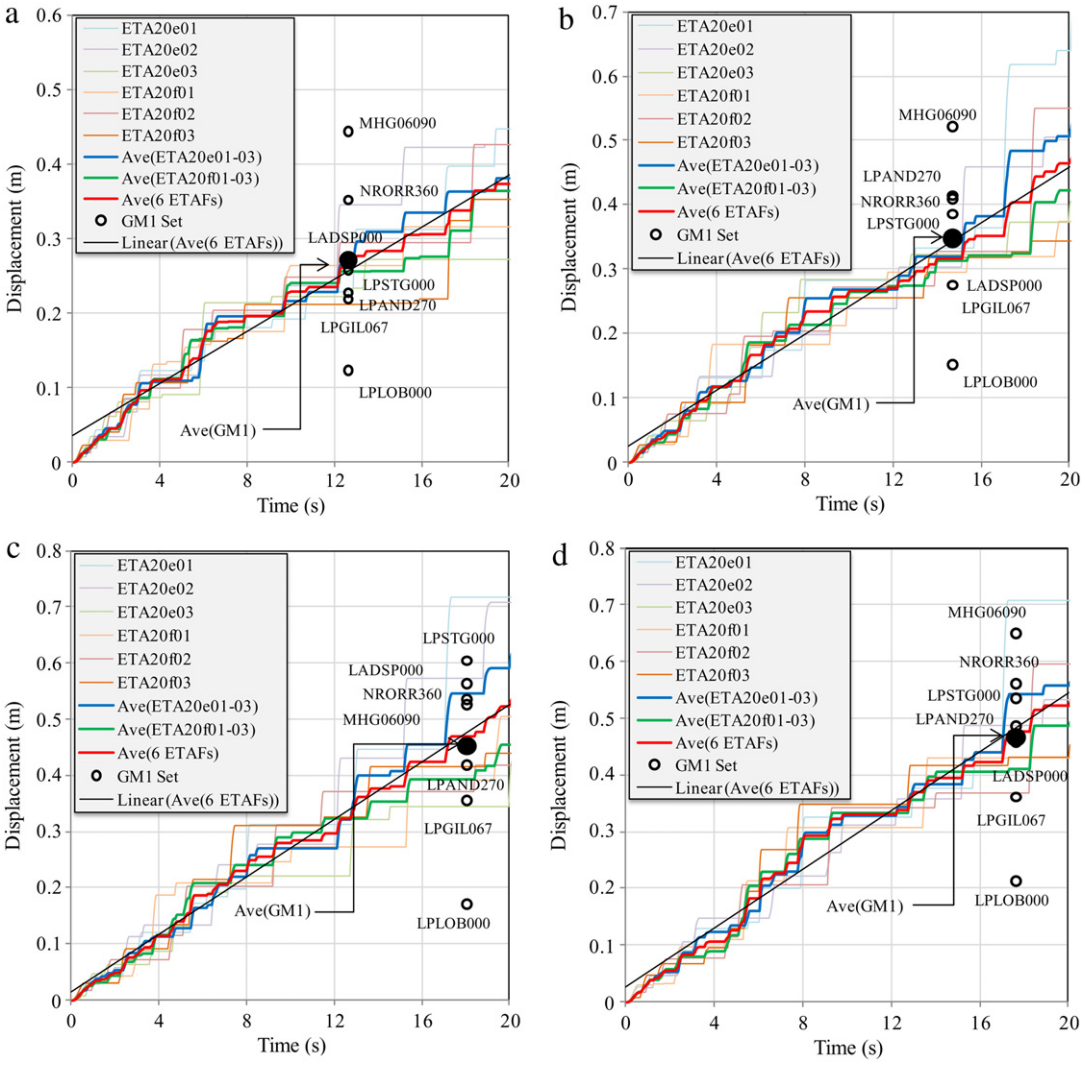

Figure 8: Comparison between roof displacement form ETA curves at equivalent target time and discrete values from real ground motions (GM1 Set), (a) SMRF09@3, $t_{eq} = 12.64$ s (b) SMRF11@3, $t_{eq} = 14.71$ s (c) SMRF13@3, $t_{eq} = 18.06$ s (d) SMRF15@3, $t_{eq} = 17.63$ s.

in which EDP_i is the value of EDP for a ground motion, n is the number of ground motions in the set, $\overline{EDP}$ is the mean value of EDP for the set, and σ is its standard deviation of it. Similar values can be calculated for the set of ETAFs. $\overline{EDP}_{ETA}$ and $\overline{EDP}_{THA}$ are maximum average results based on ETA and THA methods.

Figure 8 shows ETA curves for roof displacement and also discrete values of real ground motion in equivalent target time. In addition, the linear trend line for the ETA curve of six ETAFs is depicted in these figures. Table 3 represents the mean values and standard deviation of roof displacement between ETA and THA methods. As shown in this figure, the dispersion of results between ETAFs is less than seven ground motions. Using the average results of three or six ETAFs can effectively reduce the percentage of errors between the average of ETA and THA.

Maximum average displacement estimated by the *e*- and *f*-series, and also the GM1 set, for SMRF09@3, are 265, 265 and 270 mm. As is clear, both *e*- and *f*-series have very excellent estimation of exact displacement in this frame. Roof displacements for SMRF11@3, based on *e*-, *f*-series and the GM1 set, are 319, 313 and 347 mm, respectively, which leads to about 9% error for this frame. For SMRF13@3, maximum displacement for the mentioned dynamic loads is obtained as 545, 392 and 453 mm. As shown, using the *e*-series leads to overestimated results of about 20%. On the other hand using the *f*-series underestimates the results by about 13%, whereas using

Table 3: Comparison the results of roof displacement obtained from ETA and THA for different frames.

		Frame			
		SMRF09@3	SMRF11@3	SMRF13@3	SMRF15@3
Mean value (mm)	THA	270	347	453	466
	ETA (e-series)	265	320	545	542
	ETA (f-series)	257	313	393	410
	ETA (6 ETAFs)	260	316	469	476
Standard deviation (mm)	THA	102	122	151	143
	ETA (e-series)	70	15	188	146
	ETA (f-series)	42	17	22	36
	ETA (6 ETAFs)	51	15	146	120
Err%	ETA (e-series)	−1.85%	−7.78%	+20.31%	+16.31%
	ETA (f-series)	−4.81%	−9.79%	−13.24%	−12.01%
	ETA (6 ETAFs)	−3.70%	−8.93%	+3.53%	+2.15%

Table 4: Comparison the maximum interstory drift ratio obtained from ETA and THA for different frames.

		Frame			
		SMRF09@3	SMRF11@3	SMRF13@3	SMRF15@3
Mean value (mm)	THA	0.017	0.018	0.020	0.022
	ETA (e-series)	0.017	0.017	0.022	0.023
	ETA (f-series)	0.016	0.017	0.016	0.021
	ETA (6 ETAFs)	0.016	0.017	0.019	0.022
Standard deviation (mm)	THA	0.007	0.007	0.007	0.008
	ETA (e-series)	0.005	0.000	0.006	0.003
	ETA (f-series)	0.003	0.001	0.002	0.004
	ETA (6 ETAFs)	0.003	0.000	0.005	0.004
Err%	ETA (e-series)	0.00%	+5.56%	+10.00%	+4.55%
	ETA (f-series)	+5.88%	+5.56%	−20.00%	−4.55%
	ETA (6 ETAFs)	+5.88%	+5.56%	−5.00%	0.00%

six ETAFs as the input of the ET method, reduces errors and leads to only 3.4% error for this frame. In SMFR15@3, the results of displacement based on the e-, f-series and the GM1 set are obtained as 542, 410 and 466 mm, which leads to errors of about 16.3% and 12% using three ETAFs, whereas using six ETAFs reduces the percentage of error to only 2.1% for this frame.

Figure 9 shows that the maximum interstory drift ratio for different frames has been extracted from ground motion and ETAFs. As can be seen in this figure, in all cases, the average of interstory drift ratio extracted from the e-, f-series and the GM1 set satisfies LS performance level (below the 2.5%) and never meets CP performance level (below the 5%). Based on these results, maximum interstory drift ratio for SMRF09@3, SMRF11@3 and SMRF13@3 occurs in the middle of the frame height, as it shifts to the upper 1/3 part of the frame in SMRF15@3. Maximum interstory drift ratios for the SMRF09@3, SMRF11@3, SMRF13@3 and SMRF15@3 resulted from an average of the GM1 set are 1.61%, 1.75%, 1.99% and 2.16%. The corresponding values extracted from the e-series are 1.57%, 1.59%, 2.18% and 2.20%, and the values of the maximum interstory drift ratio from the f-series for the mentioned frames are 1.52%, 1.58%, 1.62% and 2.16%. Therefore, percentages of error between ETA and THA methods, based on using e- or f-series, are about 2.5%–5.6% for SMRF09@3, 9.1%–9.7% for SMRF11@3, 9.5%–18.5% for SMRF13@3 and 1.8%–2.3% for SMRF15@3. As clear from using three ETAFs as ETA, all percentages of error, apart from SMRF13@3, are in an acceptable range. In the case of SMRF13@3, using six ETAFs (combination of e- and f-series) leads the decreasing total errors to about 4.5%. Also, Table 4 summarizes the results of the interstory drift ratio and corresponding standard deviation for each frame.

Table 5 represents base shear for different frames extracted from THA and ETA methods. Generally, there are good consistencies between the results of the two methods. Moreover, the average results of the e- and f-series of ETAFs are very close to each other. The values of base shear for SMRF09@3, SMRF11@3, SMRF13@3 and SMRF15@3 resulted from an average of the GM1 set are 1078, 1285, 1582 and 2248 KN, respectively. The corresponding values extracted from the e-series are 1127, 1313, 1508 and 2153 KN. Values of base shear from the f-series for the mentioned frames are 1167, 1379, 1636 KN and, finally, 2140 KN. So, the percentages of error between ETA and THA methods, based on using the e- or f-series, are about 4.5%–8.2% for SMRF09@3, 2.2%–7.3% for SMRF11@3, 4.6%–3.4% for SMRF13@3 and 4.3%–4.8% for SMRF15@3. In SMRF09@3 and SMRF11@3, use of both e- and f-series leads to an overestimation of results by the ETA method, in SMRF13@3, use of the e-series leads to underestimation of results, while using the f-series leads to an overestimation of results. In SMRF15@3, both series underestimate results for base shear in comparison with the THA method. In addition, using six ETAFs in the ETA method leads to a decrease in both errors and standard deviation. Although there is no specific relation between the percentage of errors in ETA and THA methods, generally, an increase in the height of a structure leads to an increase in standard deviation in both methods.

It is noteworthy that the results of ETA are almost independent of selected records for THA, because the scaling is based on the target acceleration response spectrum. Riahi and Estekanchi [29] used another seven ground motions instead of the GM1 set for analysis of steel frames, and compared the differences of the results with those obtained from the GM1 set in order to evaluate the sensitivity of the responses to the

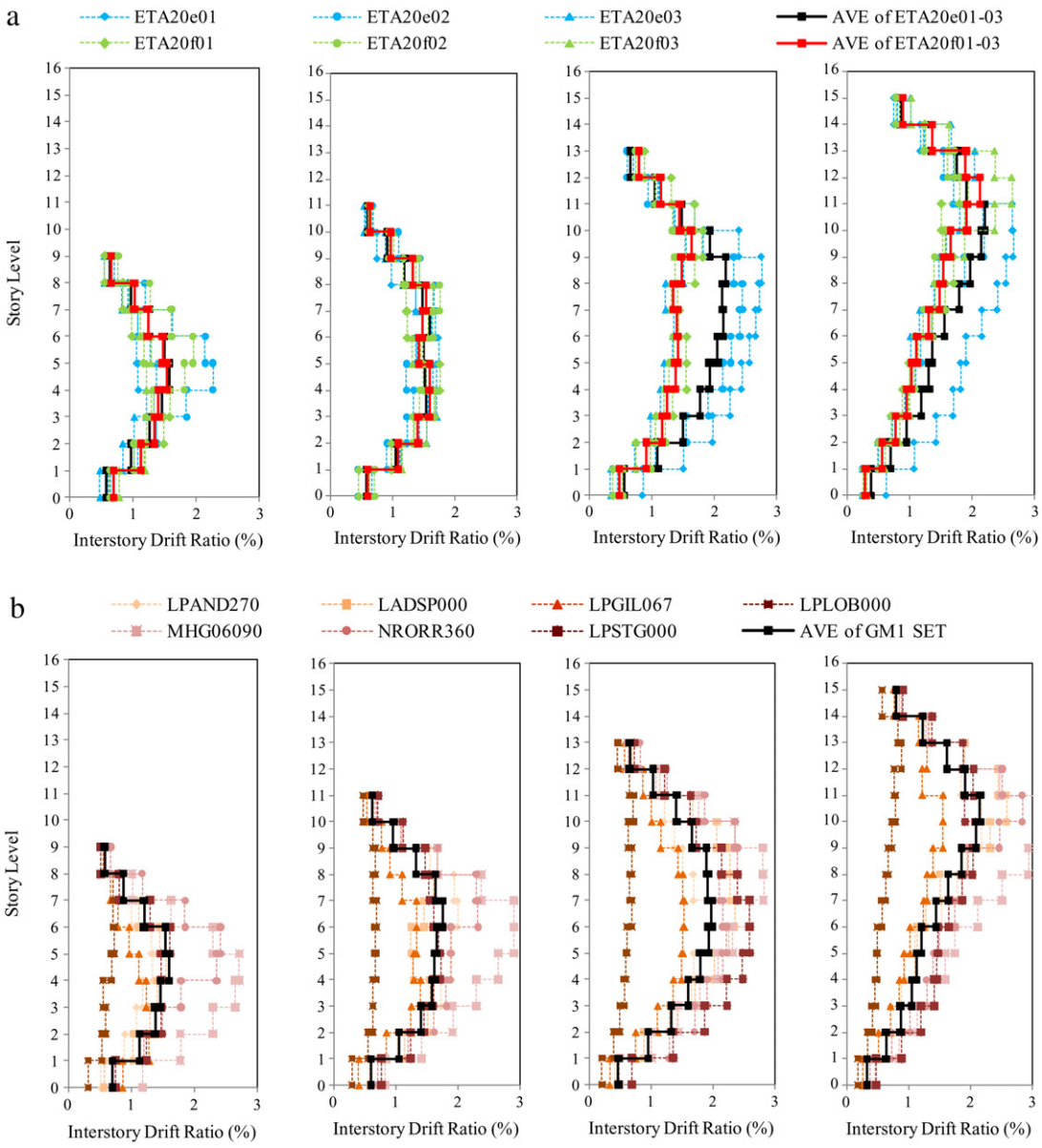

Figure 9: Maximum interstory drift ratio experienced by different stories using (a) THA method, (b) ETA method.

Table 5: Comparison the results of base shear obtained from ETA and THA for different frames.

		Frame			
		SMRF09@3	SMRF11@3	SMRF13@3	SMRF15@3
Mean value (KN)	THA	1078	1285	1582	2248
	ETA (*e*-series)	1127	1313	1509	2152
	ETA (*f*-series)	1167	1379	1636	2140
	ETA (6 ETAFs)	1148	1346	1572	2147
Standard deviation (KN)	THA	153	187	209	306
	ETA (*e*-series)	100	72	252	389
	ETA (*f*-series)	48	209	68	158
	ETA (6 ETAFs)	73	145	179	266
Err%	ETA (*e*-series)	+4.55%	+2.18%	−4.61%	−4.27%
	ETA (*f*-series)	+8.25%	+7.32%	+3.41%	−4.80%
	ETA (6 ETAFs)	+6.49%	+4.75%	−0.63%	−4.49%

Table 6: Detailed capacities for IO limit-state.

Analysis	Seismic inputs	SMRF09@3 (g)	SMRF11@3 (g)	SMRF13@3 (g)	SMRF15@3 (g)
IDA	LPAND270	1.05	1.00	1.23	1.06
	LADSP000	1.15	1.20	1.05	0.82
	LPGIL067	1.40	1.43	1.48	1.51
	LPLOB000	4.03	4.60	4.43	4.00
	MHG06090	0.55	0.62	0.71	0.61
	NRORR360	0.60	0.75	0.87	0.65
	LPSTG000	1.18	1.12	0.94	1.15
ETA	ETA20*e*01	0.91	1.14	1.14	1.14
	ETA20*e*02	0.78	1.06	1.06	1.05
	ETA20*e*03	1.35	1.39	1.38	1.14
	ETA20*f*01	1.31	1.40	1.31	1.34
	ETA20*f*02	1.37	1.37	1.37	1.37
	ETA20*f*03	1.31	1.32	1.32	1.31
	ETA20*h*01	1.44	1.43	1.71	1.44
	ETA20*h*02	1.59	1.60	1.88	1.87
	ETA20*h*03	1.88	1.50	1.50	1.50

selected ground motion. They found that although the new set (GM2) had different characteristics, the scaling procedure brings their results close together. In other words, if one target spectrum is used for scaling ground motion and calculating the equivalent time of the ETA, the results of THA and ETA will be compatible. Moreover, Hariri–Ardebili [30] investigated the capability of ETAFs in estimation of the nonlinear response of concrete arch dams, in terms of displacement and cracking pattern with site-specific real ground motion. He used ETA20e as the input of the ETA method, while he selected nine different ground motions which were not used for generation of ETAFs. He compared the results of the two methods by scaling both GMs and ETAFs based on the acceleration response spectrum of a dam at maximum credible level. He found that although there is some dispersion between the results of THA, the average results are in good agreement with those obtained from the ETA method. In both cases, the main reason for the close results between the two methods is the use of the acceleration response spectrum as an intermediate connector.

5.2. ETA vs. IDA

As mentioned above, due to the intensifying nature of ETAFs, it is possible to estimate the response of the structure at various seismic intensities in a single analysis, in this procedure. In the following subsections, the result of the ETA method in estimating various responses of a structure at different intensity levels is compared with the conventional IDA method. In the present section, another set of ETAFs are used for analysis of frames, besides the *e*- and *f*-series. This set, which is called the *h*-series, is completely similar to two previous sets in generation, but its length is double (40.96 s). Consequently, it can apply more energy to the system and lead to instability in the frames if they do not fail up to 20.48 s (maximum length of *e*- and *f*-series). On the other hand, seven ground motions of the GM1 set are used as base records in the IDA method. Although using just seven ground motions is not usual and maybe unreasonable in performance-based seismic engineering, it should be noticed that the purpose of this study is only to have a comparison between ETA and IDA methods, and also to illustrate the capability and accuracy of ETA in the estimation of structural responses at various seismic intensity levels in comparison with a set of natural ground motions. In fact, the performance of the considered frames may differ from that calculated here using a large number of ground motions. In the present study, the ETA method required only nine nonlinear analyses (three triple sets of ETAFs) in each frame, whereas the IDA method required about 200 nonlinear analyses for each to have proper estimation of frame behavior. As mentioned before, PGA was selected as IM in the present paper (another common choice for IM is 5% damped spectral acceleration at the structure's first-mode period $S_a(T_1, \xi = 5\%)$, which could be used in the present study). Considering the fact that the values of PGAs can be extracted exactly using ETAFs, while the values of $S_a(T_1, \xi = 5\%)$ at various intensities have some approximations (Eq. (3)), PGA was chosen as the base IM. It is noteworthy that based on literature, using PGA instead of $S_a(T_1, \xi = 5\%)$ can produce a higher dispersion over the full range of DM values [3], and all ground motion is scaled in the same increments (0.1 g) up to the point where instability is shown in the results. Based on the most recent research by Mirzaee et al. [31], it is possible to relate the "Time" parameter in the ETA method to a combination of the structural and return periods at different hazard curves in the IDA method using a 3D surface, in order to have better consistency between the ETA intensity parameter (Time) and conventional hazard curves. Of course, in the present paper, a similar methodology was followed, while discrete hazard levels were used instead of the continuous one, and also, the PGA was used as a correlation link between ETAFs and hazard curves instead of the spectral acceleration at specific periods or period range.

Figure 10 shows IDA and ETA curves for different frames, where DM was selected as maximum interstory drift ratio. As it can be seen in this figure, for all ground motions of the GM1 set, except LPLOB000, curves are close together. In the case of LPLOB000, the IDA curve became unstable at higher PGAs because of the very low energy of this record in the same PGA in comparison with others. In the present paper, Immediate Occupancy (IO) and Collapse Prevention (CP) were selected as structural performance levels to compare results of ETA and IDA methods. In steel moment resisting frames with type-1 connections, $\theta_{\max} = 2\%$ signifies the IO structural performance level. We also have chosen the CP point, which is thus not exceeded on the IDA/ETA curve until the final point where the local tangent reaches 20% of the elastic slope, or $\theta_{\max} = 10\%$, whichever occurs first in IM terms. Table 6 describes capacities for the IO limit-state using IDA and ETA curves. As seen, estimated capacities for the IO performance level by ETAFs are very close together. The same detailed capacities can be derived for the CP performance level as it is shown in Table 7. It is noteworthy that only the *h*-series of ETAFs can

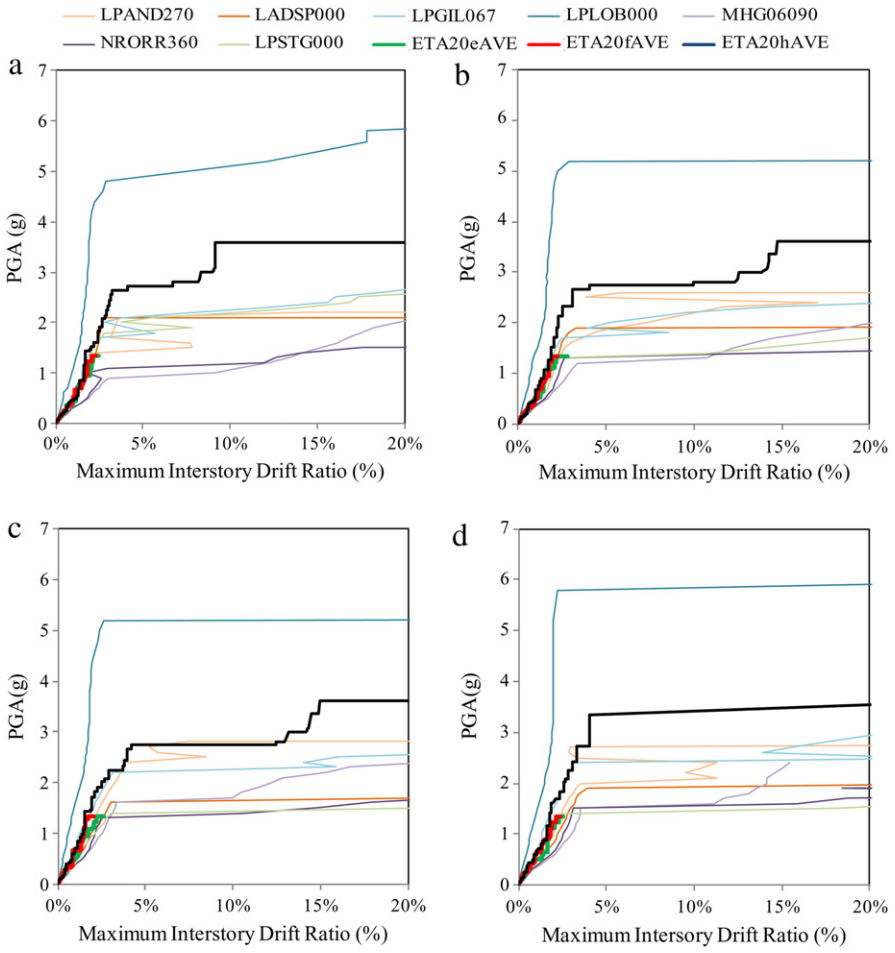

Figure 10: IDA and ETA curves for different frames using maximum interstory drift ratio as EDP (a) SMRF09@3, (b) SMRF11@3, (c) SMRF13@3, (d) SMRF15@3.

Table 7: Detailed capacities for CP limit-state.

Analysis	Seismic inputs	SMRF09@3 (g)	SMRF11@3 (g)	SMRF13@3 (g)	SMRF15@3 (g)
IDA	LPAND270	1.42	1.93	2.40	2.01
	LADSP000	2.12	1.91	1.61	1.93
	LPGIL067	1.73	1.71	2.20	2.40
	LPLOB000	4.60	5.04	5.23	5.81
	MHG06090	0.92	1.21	1.60	1.51
	NRORR360	1.12	1.30	1.30	1.51
	LPSTG000	1.82	1.31	1.40	1.41
ETA	ETA20e01	2.70	2.69	2.92	3.53
	ETA20e02	2.78	2.80	2.25	2.78
	ETA20e03	2.74	2.19	3.45	3.49

be used for determination of the collapse point in the present study, because of the short duration of the *e*- and *f*-series, the structures are not failed under these ETAFs. The limit-state capacities can be easily summarized into some central value. Consequently, we have chosen to calculate 16%, 50% and 84% fractile values of IM capacity for IO and CP limit-states, as shown in Tables 8 and 9. In addition, the last column of these tables presents the average of capacities in each frame using ETAFs.

Figure 11 shows IDA and ETA curves in which base shear was used as EDP in all cases (horizontal axis was plotted in log-scale). As can be seen, by increasing the story level, the base shear increases in both GM1 set ground motions and ETAFs. Moreover, there is very good consistency between the results of IDA and ETA methods in all cases, except LPLOB000 ground motion, which shows different behavior from other ground motions.

Table 8: Summarized capacities for IO limit-state.

	IDA			ETA
	Fractile 16% (g)	Fractile 50% (g)	Fractile 84% (g)	Average of 9 ETAFs (g)
SMRF09@3	0.56	1.15	3.29	1.32
SMRF11@3	0.66	1.12	3.71	1.36
SMRF13@3	0.75	1.05	3.60	1.41
SMRF15@3	0.62	1.06	3.30	1.35

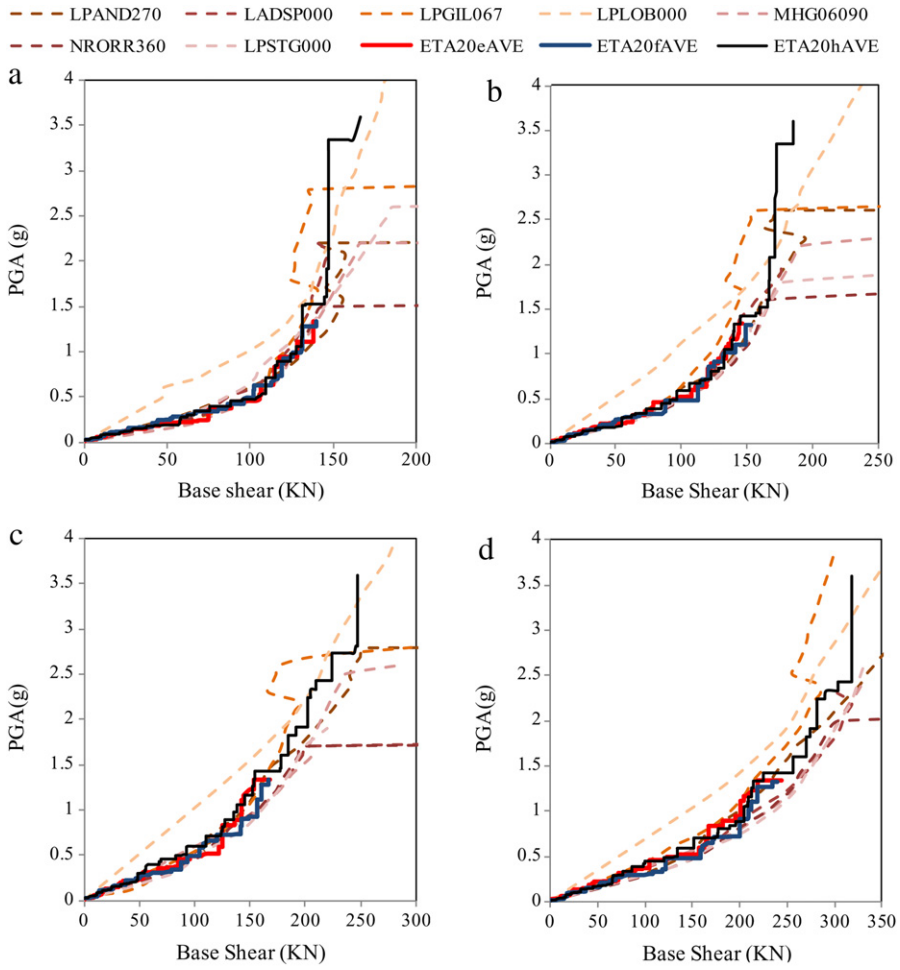

Figure 11: IDA and ETA curves for different frames using base shear as EDP (a) SMRF09@3, (b) SMRF11@3, (c) SMRF13@3, (d) SMRF15@3.

Table 9: Summarized capacities for CP limit-state.

	IDA			ETA
	Fractile 16% (g)	Fractile 50% (g)	Fractile 84% (g)	Average of 9 ETAFs (g)
SMRF09@3	0.98	1.73	3.91	2.74
SMRF11@3	1.24	1.71	4.17	2.56
SMRF13@3	1.33	1.61	4.44	2.87
SMRF15@3	1.44	1.93	4.85	3.27

5.3. Retrofitting frames

As mentioned before, with time passing, the structure experiences higher PGA and energy and, therefore, the number of elements (beams or columns) which exceed certain criteria increase. For example, in lower times, none of the beams exceeds Ratio $=$ 1 and all of them are in a safe range. Monitoring the behavior of the frame at various times under an ETAF gives appropriate information about both the location and extension of overstrain areas in the frame, and it is an effective way to find the weakest elements in the system and retrofit them. Figure 12 presents the status of beams at $t =$ 12.64 s (which is equivalent target time for SMRF09@3), and $t = 17.63$ s, (which is the equivalent target time for SMRF15@3) and also GM1 set ground motions. For SMRF09@3, the beams in all stories except the last one, exceed Ratio $=$ 1, based on both the GM1 set and ETAFs, but, as seen, there is considerable dispersion in the results of the GM1 set while using ETAFs (and also taking their average) leading to close results and smoother curves. Two other figures show the status of overstrain beams for each story in SMRF15@3. In spite of the SMRF09@3, there are two humps in the curves for SMRF15@3 and all ratios are more than one. In addition, as can be seen, using only one ETAF for the estimation of results may have considerable error, while using three ETAFs reduces error and creates good estimation of the results of real ground motion. Also, it seems that using nine ETAFs (combination of *e*-, *f*- and *h*-series) has little effect on the results, especially for mid-rise frames. By detection of overstrain elements in each frame, it is possible to retrofit the frame and weakest elements by considering dynamic loading. In other words, ETA can be used as a method for dynamic optimization and the retrofitting of structures.

6. Conclusion

In the present paper, the Endurance Time Analysis (ETA) method was introduced and its application in estimation of structural responses is compared with THA and IDA methods for SMRFs. Consequently, a set of mid-rise and high-rise frames were designed as 2D case studies for this purpose. The results of ETA using nine ETAFs were compared with the results of seven GM1 set ground motions. The average of the results in the ETA

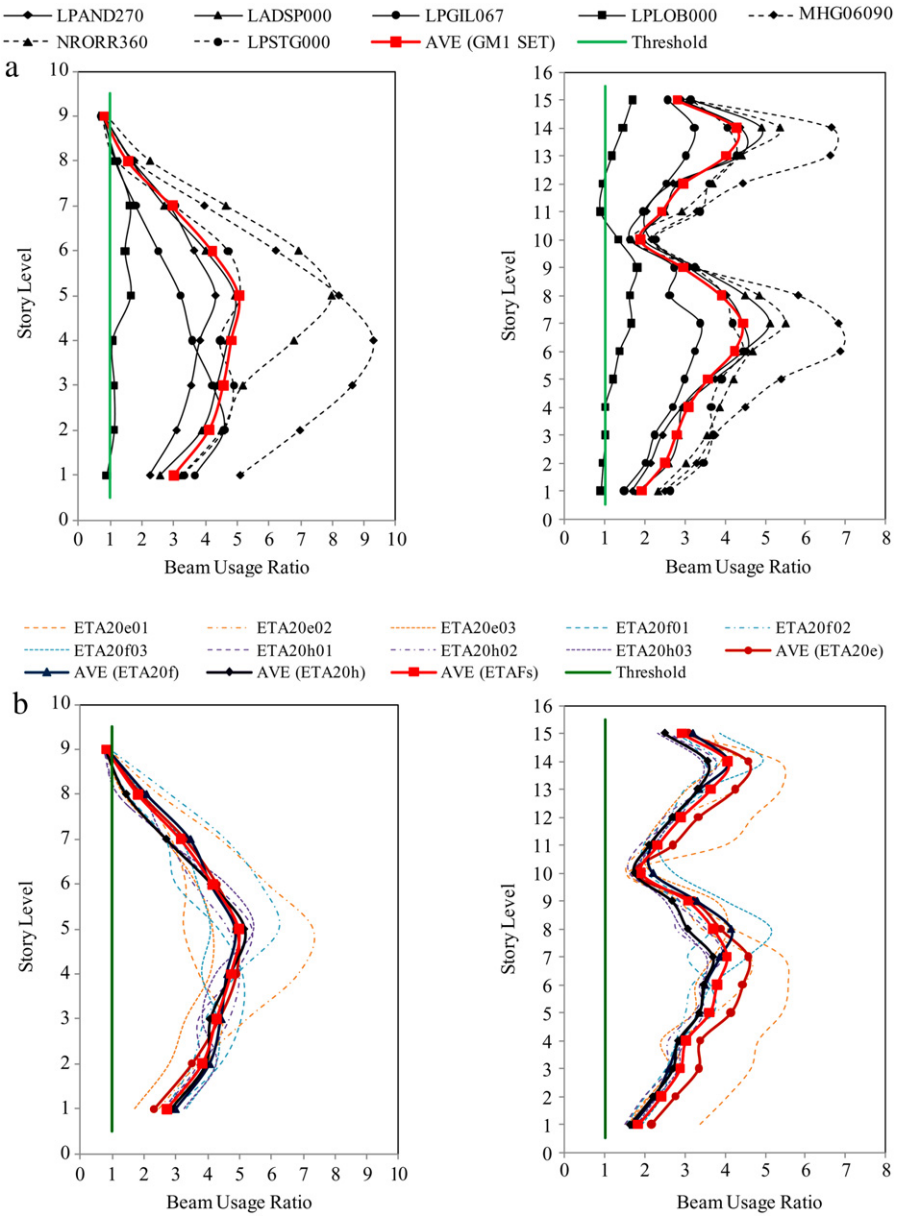

Figure 12: Overstrain beams in SCBF09@3 and SCBF15@3 frames extracted from (a) THA and (b) ETA methods.

method is approximately the same as the 50% fractile of the IDA method. Careful study of IDA and ETA curves for each frame shows that the ETA method desires to estimate the average results of ground motion with less consideration of probabilistic problems. On the other hand, study of IDA and ETA curves using the base shear as EDP shows that there is very good consistency between the two methods for different frames and at various intensity levels.

The benefit of ETA is that it estimates the response at all intensity levels in each single analysis, while both real ground motions and classically generated artificial ground motions should be scaled at each level of interest. So, the most interesting ability of the ETA method is the analysis of structural systems and the estimation of various responses with considerably low computational demand. This characteristic is important when it is required to analyse the system at different intensities, where the ETA method can give useful information about responses at various intensities with few analyses. For obtaining each IDA curve, in the present study, about 25 analyses are required and, therefore, about $7 \times 25 = 175$ analyses are needed for each frame, whereas only 9 analyses are required to obtain the results of the system based on the ETA method. This method is also capable of detecting the weakest elements and parts in the system when they are subjected to seismic input, and can be used for the retrofitting of weak and under-designed systems.

References

[1] Mwafy, A.M. and Elnashai, A.S. "Static pushover versus dynamic collapse analysis of RC buildings", *Engineering Structures*, 23, pp. 407–424 (2001).
[2] Chopra, A.K. and Goel, R.K. "A modal pushover analysis procedure to estimate seismic demands for buildings: summary and evaluation", *Proceeding of the Fifth National Conference on Earthquake Engineering*, Istanbul, Turkey, pp. 26–30 (2003).
[3] Vamvatsikos, D. and Cornell, C.A. "Incremental dynamic analysis", *Earthquake Engineering and Structural Dynamics*, 31(3), pp. 491–514 (2002).

[4] Vamvatsikos, D. and Cornell, C.A. "Applied incremental dynamic analysis", *Earthquake Spectra*, 20(2), pp. 523–553 (2004).
[5] Vamvatsikos, D. and Cornell, C.A. "Direct estimation of the seismic demand and capacity of MDOF systems through incremental dynamic analysis of an SDOF approximation", *ASCE Journal of Structural Engineering*, 131(4), pp. 589–599 (2005).
[6] Hariri-Ardebili, M.A., Zarringhalam, Y. and Yahyai, M. "Comparison of endurance time method and incremental dynamic analysis in estimation of SMRFs responses", *Proceeding of the Sixth International Conference on Seismology and Earthquake Engineering*, Tehran, Iran (2011).
[7] Hariri-Ardebili, M.A. and Mirzabozorg, H. "Estimation of concrete arch dams responses in linear domain using endurance time method", *Proceeding of the Fifth Civil Engineering Conference in the Asian Region and Australasian Structural Engineering Conference*, Sydney, Australia (2010).
[8] Estekanchi, H.E., Vafai, A. and Sadeghazar, M. "Endurance time method for seismic analysis and design of structures", *Scientia Iranica*, 11(4), pp. 361–370 (2004).
[9] Estekanchi, H.E., Valamanesh, V. and Vafai, A. "Application of endurance time method in linear seismic analysis", *Engineering Structures*, 29(10), pp. 2551–2562 (2007).
[10] Nozari, A. "Optimization of endurance time intensifying acceleration functions using classic and heuristic approaches", M.Sc. Thesis, Department of Civil Engineering, Sharif University of Technology, Tehran, Iran (2008).
[11] Nozari, A. and Estekanchi, H.E. "Optimization of endurance time acceleration functions using trust region algorithm", *Proceeding of the Sixth National Congress on Civil Engineering*, Semnan, Iran (2011).
[12] Estekanchi, H.E., Arjomandi, K. and Vafai, A. "Estimating structural damage of steel moment frames by endurance time method", *Journal of Constructional Steel Research*, 64(2), pp. 145–155 (2008).
[13] Emamjome, H. and Estekanchi, H.E. "Estimation of incremental dynamic analysis results using endurance time method", *Proceeding of the Fifth International Conference on Seismology and Earthquake Engineering*, Tehran, Iran (2007).
[14] Arjomandi, K. and Estekanchi, H.E. "A damage spectra approach to the design of steel moment frames", *Proceeding of the Fifth International Conference on Seismology and Earthquake Engineering*, Tehran, Iran (2007).
[15] Arjomandi, K. "Investigation of damage indexes in analysis of steel frames with endurance time method", M.Sc. Thesis, Department of Civil Engineering, Sharif University of Technology, Tehran, Iran (2007).
[16] Riahi, H.T., Estekanchi, H.E. and Vafai, A. "Endurance time method-application in nonlinear seismic analysis of single degree of freedom systems", *Journal of Applied Sciences*, 9(10), pp. 1817–1832 (2009).
[17] Riahi, H.T., Estekanchi, H.E. and Vafai, A. "Estimates of average inelastic deformation demands for regular steel frames by the endurance time method", *Scientia Iranica*, 16(5), pp. 388–402 (2009).
[18] Riahi, H.T. and Estekanchi, H.E. "Application of endurance time method for estimating maximum deformation demands of structures", *Proceeding of the First European Conference on Earthquake Engineering and Seismology*, Geneva, Switzerland (2006).
[19] Estekanchi, H.E., Riahi, H.T. and Vafai, A. "Endurance time method: from ideation to application", *Proceedings of a US–Iran Seismic Workshop*, Irvine, CA, USA (2009).
[20] Clough, R.W. and Penzien, J., *Dynamics of Structures*, McGraw-Hill Inc., London, UK (1993).
[21] BHRC, *Iranian Code of Practice for Seismic Resistant Design of Buildings, Standard No. 2800-05*, 3rd Edn., Building and Housing Research Center, Tehran (2005).
[22] Valamanesh, V., Estekanchi, H.E. and Vafai, A. "Characteristics of second generation endurance time acceleration functions", *Scientia Iranica*, 17(1), pp. 53–61 (2010).
[23] Federal Emergency Management Agency, "FEMA-440—Improvement of nonlinear static seismic analysis procedures", Washington DC, USA (2005).
[24] Valamanesh, V. and Estekanchi, H.E. "A study of endurance time method in the analysis of elastic moment frames under three-directional seismic loading", *Asian Journal of Civil Engineering (Building and Housing)*, 11(5), pp. 543–562 (2010).
[25] Uniform Building Code, International Conference of Building Officials (1997).
[26] Federal Emergency Management Agency, "FEMA-356—Prestandard and commentary for the seismic rehabilitation of buildings", Washington DC, USA (2000).
[27] Foutch, D.A. and Shi, S. "Effects of hysteresis type on the seismic response of buildings", In *Proceedings of the Sixth US National Conference on Earthquake Engineering*, Earthquake Engineering Research Institute, Seattle, Washington, Oakland, California (1998).
[28] *Perform-3D, Nonlinear Analysis and Performance Assessment for 3D Structures, Version 4.03*, Computers and Structures, Inc., Berkeley, California (2007).
[29] Riahi, H.T. and Estekanchi, H.E. "Seismic assessment of steel frames with endurance time method", *Journal of Constructional Steel Research*, 66(6), pp. 780–792 (2010).
[30] Hariri-Ardebili, M.A. "Estimation of probable damages in arch dams subjected to strong ground motions using endurance time acceleration functions", In *Proceeding of the Dam Safety 12 Conference*, Denver, Colorado, USA (2012).
[31] Mirzai, A., Estekanchi, H.E. and Vafai, A. "Improved methodology for endurance time analysis: from time to seismic hazard return period", *Scientia Iranica*, 19(5), pp. 1180–1187 (2012).

Mohammad Amin Hariri-Ardebili was born in 1985. He received B.S. and M.S. degrees in Civil Engineering from K.N.Toosi University of Technology, Tehran, Iran, in 2007 and 2010, respectively, and is currently pursuing his Ph.D. in Structural Engineering and Mechanics at the University of Colorado, Boulder, USA. His research interests include: concrete dam engineering; advanced dynamic of structures and PBEE; coupled system mechanics; and concrete constitutive models. He is a member of several professional institutions, such as ACI, USSD, ASDSO, S.M.ASCE, and EERI.

Yashar Zarringhalam was born in 1983. He received his M.S. degree in Earthquake Engineering from K.N.Toosi University of Technology, Tehran, Iran, in 2010, and is currently lecturer at PNU. His research interests include: performance-based design in earthquake engineering; seismic evaluation and retrofitting of building; nonlinear analysis of structures; active and passive control of structures. He has published more than 10 international conference and journal papers, as well as two books.

Homayoon E. Estekanchi is Professor of Civil Engineering at Sharif University of Technology, Tehran, Iran. He is member of the Iranian Construction Engineers Organization, ASCE, Iranian Inventors Association and several other professional institutions. His research interests include a broad area of topics in structural and earthquake engineering, with special focus on the design of tall buildings and industrial structures, and the development of a new seismic analysis and design procedure called the "Endurance Time Method" and its application on various types of structure.

Mahmood Yahyai is Associate Professor of Civil Engineering at K.N. Toosi University of Technology, Tehran, Iran. His research interests include: the dynamics of structures and earthquake engineering, wind engineering, numerical methods in structural engineering, and structural fire engineering, in which area, in collaboration with colleagues and students, he has published various research articles.